USF1 modulates transcription and cellular functions by regulating multiple transcription factors in Huh7 cells

YAN-LI ZENG[1-3], FEI GAO[1], CAN ZHANG[1], PEI-PEI REN[1], LI MA[1],
XIN WANG[4], RUZHEN WANG[1], YI KANG[1] and KE LI[1]

[1]Department of Infectious Diseases, Henan Key Laboratory for Infectious Diseases, Henan Provincial People's Hospital;
[2]Department of Infectious Diseases, Zhengzhou University People's Hospital; [3]Department of Infectious Diseases, Henan University People's Hospital; [4]Department of Infectious Diseases, Henan University, Zhengzhou, Henan 450003, P.R. China

Abstract. Liver cancer, including hepatocellular carcinoma (HCC), is a malignant tumor that has high rates of metastasis and mortality worldwide. Upstream transcription factor 1 (USF1) is a canonical transcription factor (TF) and is associated with the pathogenesis of several cancers, but its biological functions and molecular targets in HCC remain unclear. Huh7 cells that overexpress USF1 were used with whole transcriptome profiling through RNA sequencing and chromatin immunoprecipitation (ChIP) sequencing methods to investigate the downstream targets of USF1. Reverse transcription-quantitative PCR was then used to validate the downstream targets. The results showed that USF1 significantly regulates 350 differentially expressed genes (DEGs). The upregulated DEGs were primarily protein-coding genes enriched in immune and inflammation response pathways, while the downregulated DEGs were mainly coding long non-coding (lnc)RNAs, indicating the regulatory function of USF1. It was also demonstrated that USF1 directly binds to the promoter region of 2,492 genes, which may be involved in the viral progression and cell proliferation pathways. By integrating these two datasets, 16 overlapped genes were detected, including downregulated lncRNA-NEAT1 and upregulated TF-ETV5. The downregulated lncRNA-NEAT1 showed reverse expression pattern and prognosis result compared with that of USF1 in patients with liver cancer, while upregulated TF-ETV5 showed consistent results with USF1. Promoter region motif analysis indicated that ETV5 has more binding motifs and genes than USF1 itself for USF1-regulated DEGs, indicating that USF1 may indirectly modulate gene expression by regulating ETV5 expression in Huh7 cells. The study also validated the direct interaction between USF1 and the promoter of ETV5 using ChIP-qPCR. In summary, the results demonstrated that USF1 binds to the promoter region of thousands of genes and affects a large part of DEGs indirectly. Downstream genes, including lncRNA-NEAT1 and TF-ETV5, may also have potential functions in the regulated network by USF1 and have potential functions in the progression of HCC. The present findings suggested that USF1 and its downstream targets could be potential targets for HCC therapy in the future.

Introduction

Liver cancer is one of the tumors with the highest mortality rate worldwide. According to the latest Cancer Statistical yearbook, 830,000 individuals succumbed to liver cancer worldwide in 2020, accounting for 8.3% of all cancer deaths, second only to lung cancer (1). Likewise, China is also characterized by a high incidence of liver cancer and related mortality. Among all the new cases of liver cancer and liver cancer-related deaths registered worldwide, ~50% of them occurred in China, accounting for 409,000 and 391,000, respectively, and ranking second only to lung cancer in China (2). The high incidence and mortality of liver cancer pose a serious disease burden on the country and its population. Tumor resection, local ablation or liver transplantation can be used for the early treatment of liver cancer, while there is no effective treatment for advanced liver cancer due to liver metastasis. Although chemotherapy or multikinase inhibitors show some positive effects on patient survival, the prognosis remains poor (3); therefore, it is urgent to deeply analyze the pathogenesis and treatment of liver cancer (4).

Upstream transcription factor (USF) 1 belongs to the basic helix-loop-helix leucine zipper family and serves as a cellular transcription factor (TF). As a TF, USF1 has a bidirectional regulatory function, being able to regulate gene expression by activating or suppressing the promoter region of target genes (5,6). For instance, a previous study by the authors validated that USF1 binds to the core promoter of APOBEC3G and increases its transcription level in hepatocytes (7). Furthermore, it has been demonstrated that the binding of

Correspondence to: Dr Ke Li, Department of Infectious Diseases, Henan Key Laboratory for Infectious Diseases, Henan Provincial People's Hospital, 7 Weiwu Road, Zhengzhou, Henan 450003, P.R. China
E-mail: like374@163.com

USF1 to the Chitinase 3-Like 1 (Chi3L1) promoter region can enhance the transcriptional activity of Chi3L1. However, paradoxically, USF1 reduces the expression of Chi3L1 in both mouse lung tissue and human lung cancer cells (8). USF (including USF1 and USF2) is a negative transcriptional suppressor of human telomerase reverse transcriptase (hTERT) in oral cancer cells, which exerts its inhibitory effect by directly binding to the E-box site of the hTERT promoter. Loss of USF's inhibitory effect on hTERT expression may induce the reactivation of telomerase and the occurrence of oral cancer (9). The defective expression of USF1 in gastric cancer could drive p53 degradation during *Helicobacter pylori* infection and is associated with gastric carcinogenesis (10). USF1 is involved in signaling pathways, including NF-κB and inflammatory signaling (11,12). In addition to regulating the expression of protein-coding genes, USF1 can also regulate long non-coding (lnc)RNA and micro (mi)RNA that are involved in cancer development and other diseases (13,14). For example, USF1 can directly bind to the promoter region of lncRNA GAS6-AS2 and overexpress GAS6-AS2, thereby promoting the progression of osteosarcoma (13). Single nucleotide polymorphism of rs2516839 in the 5' untranslated region of USF1 is significantly associated with an increased risk of liver cancer (15). LncRNA TUG1 could recruit USF1 protein and enhance its transcriptional function activity to increase ROMO1 expression and finally promote the growth and metastasis of Huh7 cells (16). Meanwhile, USF1 promotes the expression of lncRNA-FASRL by super-enhancer, and the latter could promote *de novo* fatty acid biosynthesis to exacerbate hepatocellular carcinoma (HCC) (17). USF1 expression is increased in patients with liver cirrhosis, poorly differentiated tissues, advanced stage and metastatic recurrence, suggesting its potential as a novel marker for metastatic recurrence in patients with liver cancer (18).

To investigate the clinical role of USF1 and elucidate the mechanisms involving genome-wide USF1 binding sites and downstream gene alterations in cancer, the present study followed a comprehensive research approach. The study first examined the correlation between USF1 expression and patient prognosis within a tissue microarray cohort. This initial analysis was aimed to determine whether a significant association exists between USF1 expression levels and clinical outcomes in cancer. Subsequently, chromatin immunoprecipitation followed by high-throughput sequencing (ChIP-seq), a cutting-edge technique enabling the high-resolution, genome-wide identification of DNA-binding protein sites was employed to precisely pinpoint the binding sites of the USF1 protein throughout the entire genome. To further advance the present research, cellular models involving USF1 overexpression (USF1-OE) were established. Finally, RNA-sequencing (RNA-seq) was used to obtain transcriptomic data. This approach allowed a comprehensive investigation of the impact of USF1 on gene expression and function at the genomic level.

Materials and methods

Cloning and plasmid construction. The pcDNA3.1-USF1 (cat. no. NM_007122) plasmid was purchased from Youbio Biotech (Changsha, China).

Cell culture and transfections. Huh7 cells, an adult HCC cell line (cat. no. CL-0120; Procell Life Science & Technology Co., Ltd.), were cultured at 37˚C with 5% CO_2 in DMEM (cat. no. PM150210; Procell Life Science & Technology Co., Ltd.) with 10% FBS (cat. no. 10091148; Gibco; Thermo Fisher Scientific, Inc.), 100 μg/ml streptomycin and 100 U/ml penicillin (cat. no. SV30010, HyClone; Cytiva). For USF1-OE, 500 ng empty plasmid or USF1 overexpression plasmid were transfected into Huh7 cells at 37˚C using Lipofectamine™ 2000 (cat. no. 11668019; Invitrogen; Thermo Fisher Scientific, Inc.) for 48 h, according to the manufacturer's protocol. The plasmid backbone used was pcDNA 3.1-C-FLAG, purchased from Youbio. The transfected cells were harvested for reverse transcription-quantitative (RT-q) PCR and western blotting analyses 1 week after transfection.

Western blotting. Huh7 cells were lysed in ice-cold RIPA buffer (cat. no. PR20001; Wuhan Sanying Biotechnology) supplemented with a protease inhibitor cocktail (cat. no. 4693116001; Sigma-Aldrich; Merck KGaA) and incubated on ice for 30 min. Samples were kept for 10 min in boiling water with protein loading buffer (cat. no. P1040; Beijing Solarbio Science & Technology Co., Ltd.). A total of 25 μg protein (as determined by the BCA method) was loaded per lane of a 10% gel and the proteins were separated by SDS-PAGE, then transferred onto 0.45-mm PVDF membranes (cat. no. ISEQ00010; MilliporeSigma). The PVDF membranes were then blocked using 5% skim milk for 1 h at room temperature and incubated overnight at 4˚C with primary antibody against FLAG tag (anti-FLAG; 1:2,000; antibody produced in rabbit; cat. no. F7425; Sigma-Aldrich; Merck KGaA) and GAPDH (1:1,000; antibody produced in rabbit; cat. no. A19056; ABclonal Biotech Co., Ltd.), followed by an incubation with horseradish peroxidase-conjugated secondary antibody (anti-rabbit; 1:5,000, cat. no. SA00001-2; Wuhan Sanying Biotechnology) or anti-mouse, 1:5,000; cat. no. AS003; ABclonal Biotech Co., Ltd.) for 45 min at room temperature. Subsequently, the protein bands on the membranes were visualized through chemiluminescence using ECL reagent (cat. no. P0018FM; Beyotime Institute of Biotechnology).

RNA-seq and data analysis. RNA-seq assays were performed by Wuhan Ruixing Biotechnology Co., Ltd. (http://www.rxbio. cc). The collected Huh7 cells were subjected to total RNA extraction using TRIzol® (cat. no. 15596-018, Ambion; Thermo Fisher Scientific, Inc.). The total RNA was further purified with two phenol-chloroform treatments and then treated with RQ1 DNase (cat. no. M6101; Promega Corporation) to remove DNA. The quality and quantity of the purified RNA were determined by measuring the ratio of the absorbances measured at 260 and 280 nm (A260/A280=1.9-2.1) using an Ultrafine spectrophotometer (N50 touch; Implen GmbH). The integrity of RNA was further verified using 1.5% agarose gel electrophoresis followed by staining with gel red (cat. no. GR501-01; Vazyme Biotech Co., Ltd.) for visualization. For each sample, 1 μg of the total RNA was used for RNA-seq library preparation using the VAHTS Stranded mRNA-seq Library Prep kit (cat. no. NR605-02, Vazyme Biotech Co., Ltd.). Polyadenylated mRNAs were purified and fragmented, and then converted

into double-strand cDNA. After end repair and A tailing, the DNAs were ligated to VAHTS RNA Adapters. Purified ligation products corresponding to 200-500 bps were digested with heat-labile uracil-DNA glycosylase and the single-strand cDNA was amplified, purified, quantified and stored at -80°C before sequencing. For high-throughput sequencing, the libraries were prepared following the manufacturer's instructions and applied to the Illumina Nova6000 system (Illumina, Inc.) for 150 nt paired-end sequencing.

For data analysis, raw reads containing >2-N bases were first discarded, and then adaptors and low-quality bases were trimmed from raw sequencing reads using the FASTX Toolkit (Version 0.0.13; hannonlab.cshl.edu/fastx_toolkit/). The short reads <16 nt were also dropped. After that, clean reads were aligned to the human GRCh38 genome using HISAT2 (version 2.2.1) (19) allowing no more than four mismatches. Uniquely mapped reads were used for gene reads number counting and fragments per kilobase of transcript per million fragments mapped (FPKM) (20). The R Bioconductor package 'edgeR' (21) was utilized to screen out the differentially expressed genes (DEGs). P<0.01 and fold change >2 or <0.5 were set as the cut-off criteria for identifying DEGs.

ChIP-seq and data analysis. ChIP assay was performed by Wuhan Ruixing Biotechnology Co., Ltd. (http://www.rxbio.cc). A total of ~1×10^7 cells were crosslinked in 1% formaldehyde for 10 min and the reaction was quenched with 0.125 M glycine for 5 min at room temperature. The cross-linked cells were lysed in Lysis buffer (1X PBS, 0.1% SDS, 0.5% NP-40 and 0.5% sodium deoxycholate) and sonicated to generate DNA fragments of 200-1,000 bp in length. For immunoprecipitation, protein-DNA complex was immunoprecipitated by incubating with ChIP-grade Protein A/G Magnetic Beads (50 μl for IP and 10 μl for IgG; cat. no. 26162; Invitrogen; Thermo Fisher Scientific, Inc.) conjugated with anti-FLAG antibody (cat. no. F7425; Sigma-Aldrich; Merck KGaA), or IgG (cat. no. B900610; Wuhan Sanying Biotechnology) at 4°C for 2 h. The beads were washed with LiCl Immune Complex wash buffer (0.5 M LiCl) five times, and TE buffer [10 mM Tris (pH 8.0), 1 mM EDTA (pH 8.0)] for one time. The beads were resuspended with 100 μl Elution Buffer (100 mM NaHCO$_3$ and 1% SDS) and reverse cross-linked by overnight incubation at 65°C. After sequential RNase A and proteinase K treatments, DNA fragments were purified through phenol extraction and ethanol precipitation. The libraries were performed by using VAHTS Universal DNA Library Prep Kit for Illumina V3 (cat. no. ND607; Vazyme Biotech Co., Ltd.), according to the manufacturer's instructions, and PCR products corresponding to 200-500 bps were enriched, quantified and finally sequenced on Novaseq 6000 sequencer (Illumina, Inc.) with PE150 model. Reads were aligned to the human GRCh38 genome using bowtie2 (22). Only uniquely mapped reads were used for the following analysis. To identify the binding sites of USF1, Model-based Analysis for ChIP-seq (MACS version 1.4; https://github.com/macs3-project/MACS/blob/macs_v1) was employed (23). The input samples without immunoprecipitation were used as controls. DeepTools (Version 3.4.3) (24) was used for the assignment of genomic features, such as relative location to the transcription start site (TSS) to the peaks and visualization of binding profiles. Hypergeometric Optimization of Motif Enrichment (HOMER) software (http://homer.ucsd.

edu/homer/motif/) (25) was used to search the enriched binding motifs in peaks.

RT-qPCR and ChIP-qPCR. cDNA synthesis was performed using a reverse transcription kit (cat. no. R323-01; Vazyme Biotech Co., Ltd.) in the thermocycler T100 (Bio-Rad Laboratories, Inc.) with the following thermocycling conditions: 42°C for 5 min, 37°C for 15 min, 85°C for 5 sec. ChIP assay was performed according to the aforementioned method. The qPCR was performed on an ABI QuantStudio 5 (Thermo Fisher Scientific, Inc.) with Hieff™ qPCR SYBR® Green Master Mix (Low Rox Plus) (cat. no. Q431-02; Shanghai Yeasen Biotechnology Co., Ltd.) and the following thermocycler conditions: Denaturing at 95°C for 10 min, 40 cycles of denaturing at 95°C for 15 sec and annealing and extension at 60°C for 1 min. Each sample was analyzed in three technical replicates. The concentration of each transcript was then normalized to the internal reference gene GAPDH and mRNA levels were quantified using the $2^{-\Delta\Delta Cq}$ method (26). Comparisons were performed with the paired Student's t-test by using GraphPad Prism software (version 8.0; Dotmatics). The primer sequences for PCR experiments were provided in Table SI. Comparisons were performed with the paired Student's t-test and two-way ANOVA by using GraphPad Prism software (Version 8.0; Dotmatics). The data analyzed in the present study are available under Gene Expression Omnibus database series accession no. GSE232263.

Statistical analysis. Expression and prognosis analyses of genes from patients with liver hepatocellular carcinoma (LIHC) were performed using Gene Expression Profiling Interactive Analysis 2 (GEPIA2) online server (27) and Kaplan-Meier (K-M) Plotter webpage, respectively (28). Principal component analysis (PCA) was performed with the R package 'factoextra' (https://cloud.r-project.org/package=factoextra). The 'pheatmap' and 'ggplot2' packages (https://cran.r-project.org/web/packages/) in R were used to generate figures.

Results

USF1 is highly expressed in patients with liver cancer and is associated with prognosis. To explore the clinical influence of USF1 in liver cancer, its expression pattern and prognostic effect were investigated by analyzing data retrieved from The Cancer Genome Atlas (TCGA) database using GEPIA2 and K-M Plotter software, respectively. A significant increase in USF1 expression level was observed in LIHC compared with that in normal samples (Fig. 1A). Expression pattern sorted by tumor stages showed that the USF1 expression level was high in stage I-III while it decreased in stage IV (Fig. 1C). Meanwhile, patients with higher expression of USF1 showed worse prognosis than patients with a lower level of USF1 (Fig. 1B). These results indicate that USF1 influences the clinical features of patients with liver cancer and the underlying mechanisms should be further investigated.

Construction of Huh7 cell line overexpressing USF1 and following RNA-seq analysis. To further explore the molecular mechanisms of USF1 in liver cancer cells, Huh7 cells were transiently transfected with USF1-OE plasmid to construct
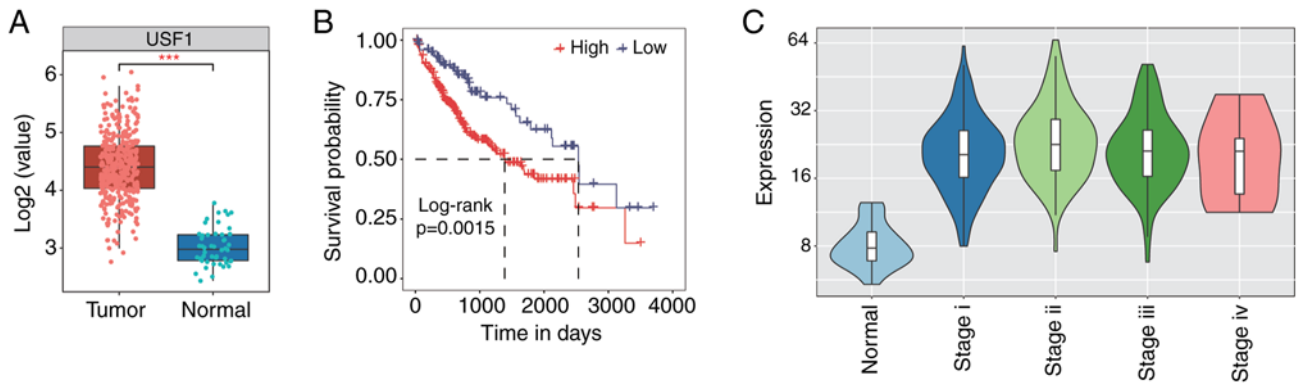
Figure 1. USF1 is highly expressed in patients with LIHC and associated with poor prognosis of LIHC patients. (A) Box plot showing the expression level of USF1 in LIHC patients. [***]P<0.001 by t-test. (B) Line plot showing the prognostic results by dividing LIHC patients into two groups according to USF1 expression levels. (C) Violin plot showing the expression level change of USF1 by the LIHC stages. USF1, upstream transcription factor 1; LIHC, liver hepatocellular carcinoma.
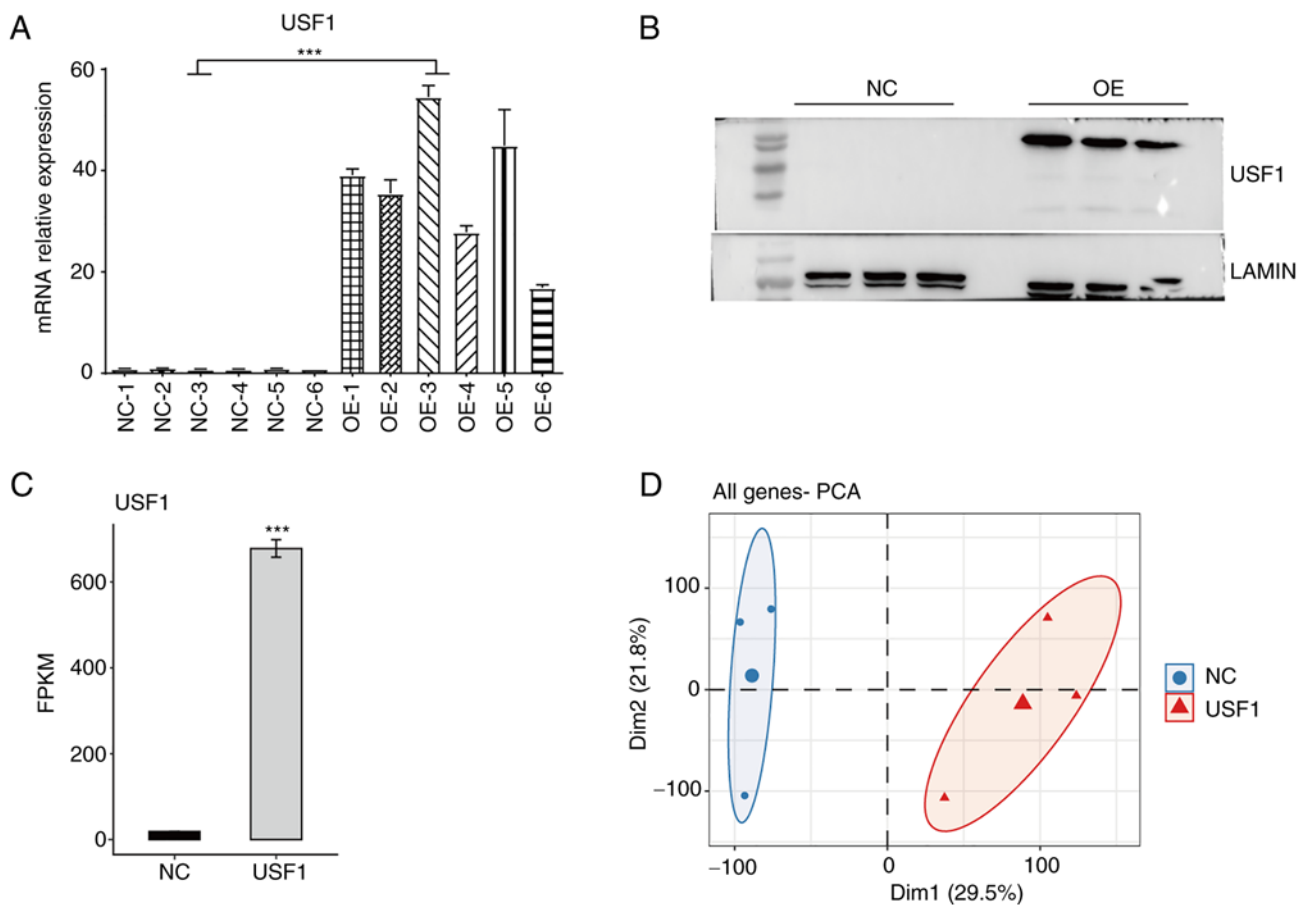

Figure 2. USF1-OE globally modulates the transcriptome profile of Huh7 cells. (A) Bar plot showing the reverse-transcription quantitative PCR result for USF1-OE in Huh7 cells. (B) Western blotting result showing the successful overexpression of USF1 in Huh7 cells. (C) Bar plot showing the FPKM values of USF1 in Huh7 cells. (D) PCA result showing the clear separation between USF1-OE and control samples. [***]P<0.001 by two-way ANOVA. USF1, upstream transcription factor 1; OE, overexpression; FPKM, fragments per kilobase of transcript per million fragments mapped; PCA, Principal component analysis; NC, negative control.

USF1-OE Huh7 cells. The overexpression efficiency was confirmed using RT-qPCR and western blotting. The RT-qPCR results showed that the mRNA levels of USF1 in USF1-OE Huh7 cells were >15 times higher than that in normal Huh7 cells (Fig. 2A) and the western blotting results revealed that the protein levels of USF1 were also increased

(Fig. 2B). RNA-seq experiments were then performed to identify the genes differentially expressed by USF1-OE in Huh7 cells. After aligning quality-filtered reads onto the human genome, the expression levels of all detected genes were obtained. Compared with the control cells, the FPKM value of USF1 in USF1-OE cells significantly increased from
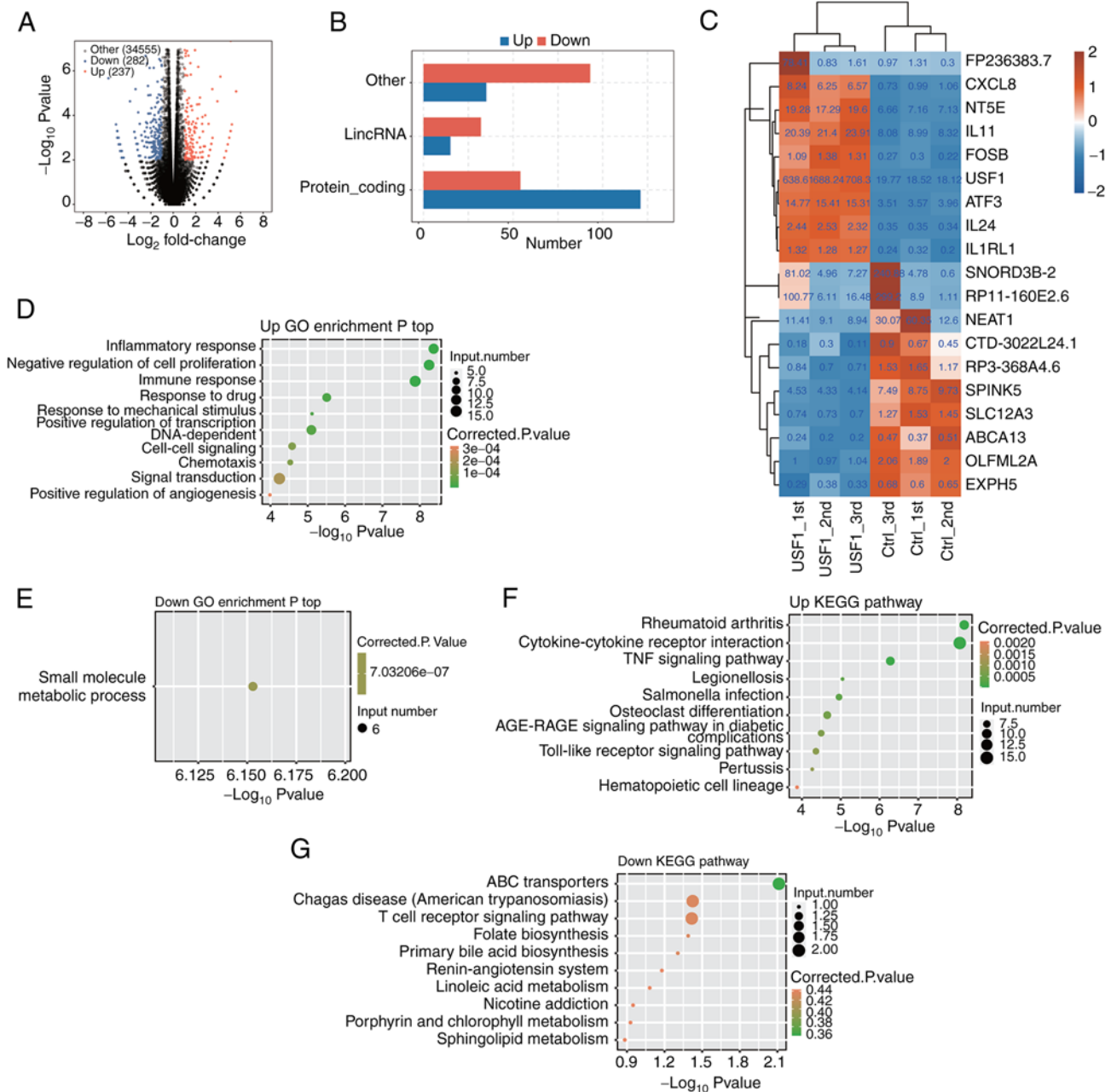
Figure 3. USF1-regulated DEGs are enriched in immune and cell proliferation associated pathways. (A) The DEGs were presented by volcano plot. Red and blue points were upregulated and downregulated DEGs, respectively. (B) Bar plot showing the RNA types of upregulated and downregulated DEGs. (C) Hierarchical clustering heatmap showing the expression pattern of top 10 upregulated DEGs and downregulated DEGs that were sorted by adjusted P-value. (D) Bubble plot showing the top ten enriched BP pathways for upregulated DEGs regulated by USF1-OE. (E) Bubble plot showing the only one enriched BP pathway for down DEGs regulated by USF1-OE. (F) Bubble plot showing the top ten enriched KEGG pathways for upregulated DEGs regulated by USF1-OE. (G) Bubble plot showing the top ten KEGG pathways for downregulated DEGs regulated by USF1-OE. USF1, upstream transcription factor 1; DEGs, differentially expressed genes; OE, overexpression; BP, Biological Process; KEGG, Kyoto Encyclopedia of Genes and Genomes; GO, Gene Ontology.

18.80 to 678.38 (Fig. 2C), indicating that the experiment was successful. PCA of all expressed genes demonstrated the clear separation between USF1-OE and control cells (Fig. 2D). These results demonstrated that the USF1-OE cell line was successfully constructed, and it was found that USF1-OE globally regulates the transcriptome profile of Huh7 cells.

Analyses of DEGs in USF1-OE Huh7 cells. To explore genes that USF1 may regulate, RNA-seq was used to characterize the changes in gene expression in Huh7 cells after USF1 OE. The results showed that there were 350 DEGs after USF1-OE, including 171 upregulated and 179 downregulated genes (Fig. 3A). From the numbers of upregulated and downregulated genes, there were no significant differences in USF1 promoting or restraining gene expression. However, regarding the types of genes, there were significant differences. The most upregulated genes were protein-coding genes, and TFs, while the most downregulated genes were long intergenic non-coding (linc)RNAs and other types (Fig. 3B), indicating that USF1 could activate the expression of protein-coding genes. The changes in the expression level of the top 10 upregulated and downregulated genes were then shown. USF1 displayed the
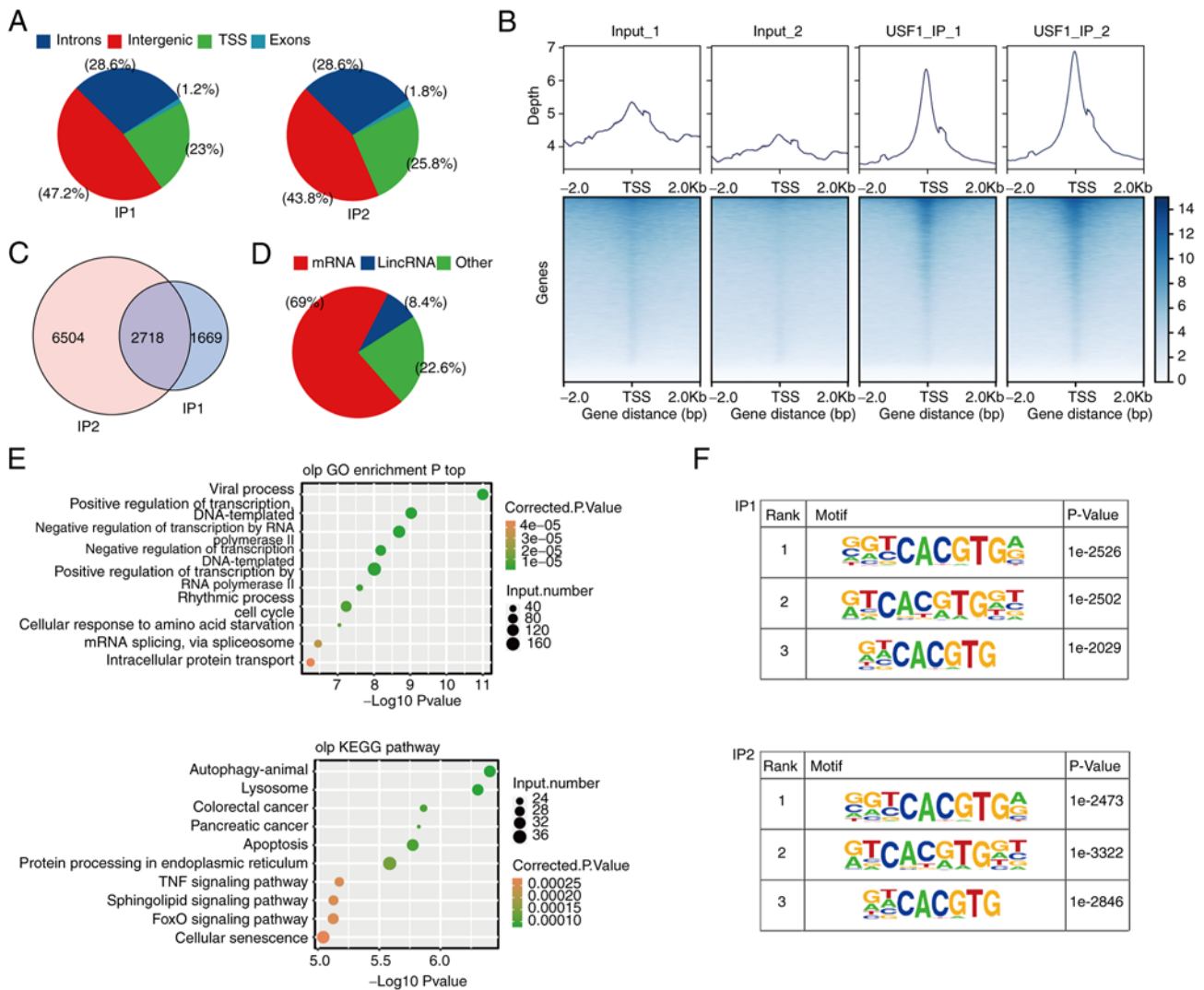
Figure 4. USF1 extensively binds to the promoter of genes that are associated with cancer development. (A) Pie chart showing the genomic region distribution of mapped reads from USF1 Chromatin Immunoprecipitation-sequencing data. (B) Density and heatmap plot showing the binding profiles around TSS region for all genes in Input and USF1 IP samples. (C) Venn diagram showing the overlapped genes between IP1 and IP2 samples. (D) Pie chart showing the RNA types for the transcripts of USF1-bound genes. (E) Bubble plot showing the enriched GO BP (top panel) and KEGG (bottom panel) pathways for USF1-bound genes. (F) The detected motifs from the two USF1 IP samples. USF1, upstream transcription factor 1; TSS, transcription start site; IP, immunoprecipitation; GO, Gene Ontology; BP, Biological Process; KEGG, Kyoto Encyclopedia of Genes and Genomes.

most significant upregulation, whereas the lincRNA NEAT1 exhibited the most pronounced downregulation. Notably, the extent of change in NEAT1 expression was comparatively less than that observed for USF1 (Fig. 3C).

Subsequently, the enriched functions of upregulated and downregulated DEGs which were found following USF1-OE were analyzed. USF1-OE led to the upregulation of several inflammation and immune-associated pathways, including inflammatory response, immune response, signal transduction and negative regulation of cell proliferation (Fig. 3D). Surprisingly, most of the downregulated genes were only enriched in one biological process pathway (small molecule metabolic process; Fig. 3E), which may be attributed to the less protein-coding genes among downregulated DEGs. Kyoto Encyclopedia of Genes and Genomes (KEGG) analysis showed that upregulated genes were also mainly related to signaling pathways, including the TNF signaling pathway, AGE-RAGE signaling pathway and Toll-like receptor

signaling pathway (Fig. 3F). The downregulated genes were enriched in ABC transporters, Chagas disease, T cell receptor signaling pathway and other pathways (Fig. 3G). These results demonstrated that USF1-OE mainly regulates the expression of immune/inflammation-associated genes, as well as cell proliferation-associated genes.

Analyses of the potential gene targets of USF1. To identify the potential gene targets of USF1, ChIP-seq was used to characterize all DNA directly bound by USF1 and two replicate libraries were constructed to improve accuracy. The results demonstrated that most of the binding sites were in the TSS, intergenic and intron regions (Fig. 4A). The binding profile around the TSS region demonstrated that the binding peaks of USF1 were highly enriched in the TSS region (Fig. 4B). A total of 10,891 genes were involved in binding with USF1, indicating that the USF1 binding to target genes is extensive (Fig. 4C). The subsequent analysis focused on the 2,718 genes which

were detected in both sets of experiments (Fig. 4B). There was a variety of gene types in these 2,718 genes, including protein coding genes, lincRNA, microRNA, small nucleolar RNA and others, indicating that the USF1 binding targeted an extensive range of genes (Fig. 4D). Gene Ontology (GO) analysis showed that these genes were mainly related to the biological processes associated with the occurrence and development of cancer, such as apoptotic process, cell death and mitotic cell cycle (Fig. 4E). KEGG analysis showed that these genes were mainly related to signaling pathway (Sphingolipid and FoxO signaling pathways), cancer and protein processing (Fig. 4E). Subsequently, HOMER identified the potential motifs in the target sequences, revealing that the motif G(C)GTCACG TGA(G), G(A)TCACG(A)TGGT and G(A)T(A)CACGTG were the top three most frequent sequences overexpressed among the USF1-binding sites (Fig. 4F). The identified motifs were canonical cognate E-box regulatory elements of USF proteins (29).

USF1 binds to the promoter of a few genes and regulates their expression in Huh7 cells. To identify the genes which were bound and regulated by USF1, the data of RNA-seq and ChIP-seq were combined for further analysis. Only 16 genes could be bound by USF1 in 350 DGEs, including 10 protein-coding genes, three antisense genes, two lincRNA and one sense intronic gene (Fig. 5A; Table SII). The expression levels of these overlapped genes were investigated and it was found that there were only two downregulated genes, while all the remaining genes were upregulated (Fig. 5B). The results revealed that USF1 significantly binds to the promoter region of NEAT1 by exhibiting the reads density of ChIP-seq data (Fig. 5C). Meanwhile, the expression level of NEAT1 was significantly decreased by USF1 (Fig. 5D). NEAT1 is a canonical lincRNA and a novel target for diagnosis and therapy in human tumors (30). The present study further explored the expression level and prognostic influence of NEAT1 in liver cancer. Based on the TCGA LIHC RNA-seq data, the tumor samples exhibited a lower expression level of NEAT1 compared with that in normal samples (Fig. 5E). Meanwhile, the overall survival analysis by the K-M method demonstrated that patients with higher NEAT1 expression levels showed improved prognostic results compared with those patients with lower NEAT1 expression level (Fig. 5F). These results were consistent with those of USF1 demonstrated in Fig. 1 after considering that USF1 negatively regulated NEAT1 expression. In summary, the aforementioned results indicated that USF1 regulates the expression of several genes by directly binding to their promoter region and this regulation may be associated with its biological functions in liver cancer.

USF1 modulates gene expression by regulating TFs in Huh7 cells. Very few overlapped genes between USF1-bound genes and DEGs were detected, which were not significant after calculation (P=0.97, hypergeometric test). This result indicated that USF1 may indirectly regulate gene expression in Huh7 cells. To confirm this hypothesis, TFs were extracted from DEGs. Several genes among the overlapped genes were TFs, including GBX2, FOSB, ETV5 and EGR1. Among these TFs, ETV5 had the highest expression level and a significant expression increase after USF1-OE (Fig. 6A), indicating that

ETV5 may have important roles in Huh7 cells and HCC. The expression level and prognostic effect of ETV5 in patients with LIHC were investigated and it was found that the EVT5 expression was significantly increased in tumor samples (Fig. 6B), while patients with higher ETV5 expression showed worse prognosis results (Fig. 6C). ChIP-qPCR experiments validated that USF1 significantly binds to the promoter region of ETV5 (Fig. 6D and E). To further explore the underlying mechanisms of the differentially expressed TFs (DETFs), the occurrence of the motif sites of these four TFs within the promoter region of DEGs in USF1-OE Huh7 cells were analyzed to identify which TF had the highest frequency of motif sites and the number of DEGs. This analysis was also performed for USF1. The results demonstrated that EGR1 and ETV5 have the highest frequency of their motifs, which was markedly higher than that of USF1 (Fig. 6F). Although EGR1 had more motif sites than ETV5, the expression level of EGR1 in LIHC tumor samples was lower than that in normal samples (Fig. S1A), and patients with higher EGR1 expression level showed improved prognosis compared with that in patients with lower EGR1 expression level (Fig. S1B), indicating that USF1 may not promote HCC progression by mediating EGR1 expression. Furthermore, DEG number analysis of these identified motifs demonstrated that ETV5 occupies more DEGs than other TFs and USF1 (Fig. 6G), suggesting that ETV5 may regulate the expression of these DEGs and USF1 may indirectly affect gene expression by ETV5 in Huh7 cells.

Discussion

USF1 is a canonical TF that affects the expression of numerous genes by binding to their promoter region or super-enhancers to control the transcription process. Previous studies demonstrated the critical roles of USF1 in HCC exacerbation and identified several downstream targets of USF1 (16,17), while the global binding profile on DNA and the downstream-regulated genes of USF1 have not been deeply investigated in liver cancer. In the present study, whole transcriptome sequencing and ChIP-seq experiments were performed to systematically explore how USF1 affects gene expression and the biological functions of USF1 in HCC Huh7 cells. USF1 globally enhanced the expression level of immune and inflammatory-associated genes, while the downregulated genes by USF1-OE were mainly non-coding. By integrating the ChIP-seq data, it was found that USF1 may regulate the expression of a few genes by binding to their promoters, while a larger number of DEGs were not bound by USF1 and may be regulated by other DETFs, suggesting a novel regulatory mechanism of USF1 in liver cancer cells.

Consistent with a previous study (17), USF1 was upregulated and associated with a worse prognosis in patients with LIHC. To explore the underlying mechanisms, USF1 was overexpressed in Huh7 cells and DEGs were identified. Interestingly, DEGs upregulated by USF1-OE were significantly enriched in inflammatory and immune response pathways. It was also demonstrated that USF1 promotes TNFAIP3/A20 expression, and thus inhibits inflammatory NF-κB pathway activity; this regulatory axis is a potential anti-inflammatory strategy for the treatment of several diseases (31). The USF1/A20 regulatory axis was also validated in mitigating vascular inflammation
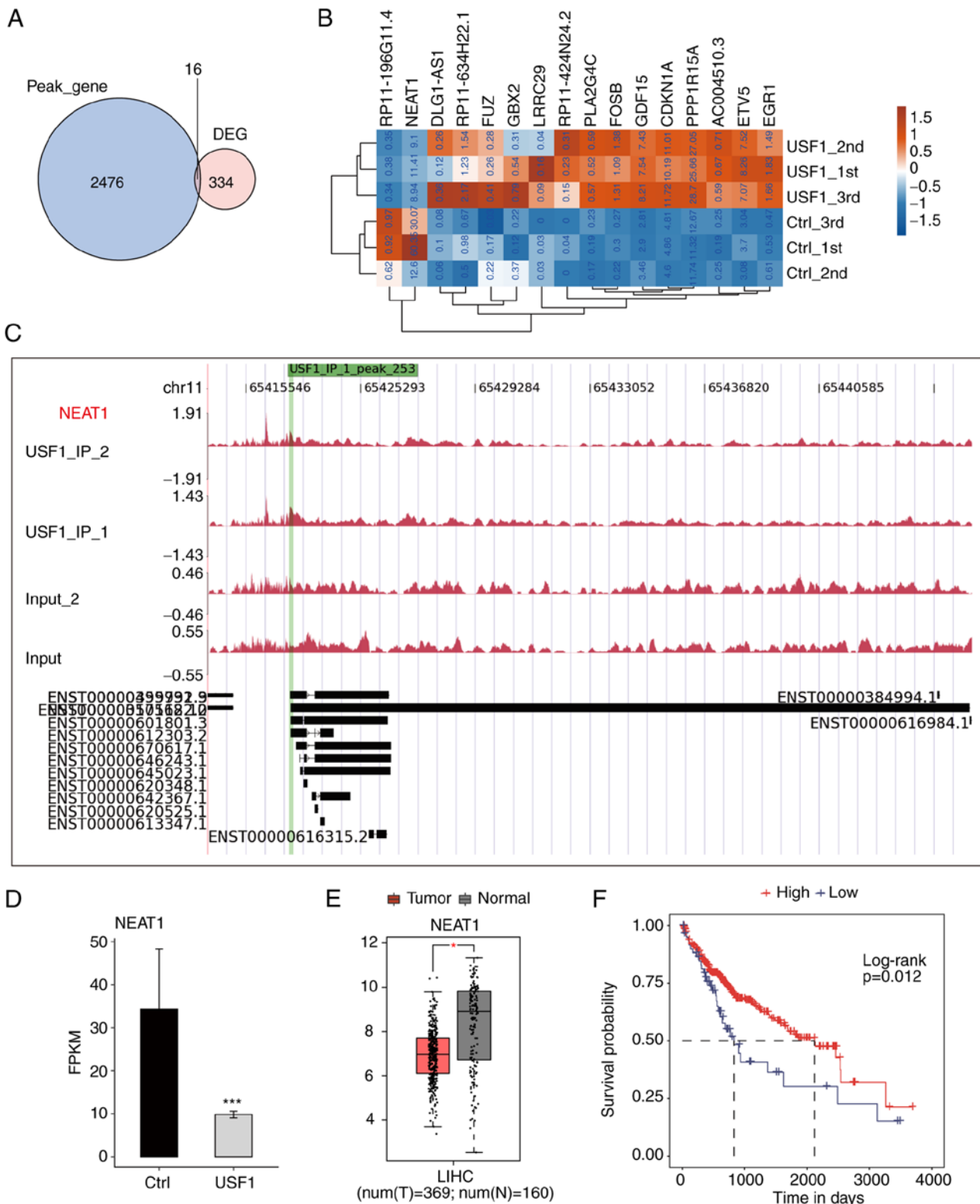
Figure 5. USF1 binds to genes to regulate their expression levels in liver cancer cells. (A) Venn diagram showing the overlapped genes between DEGs and USF1-bound genes. (B) Hierarchical clustering heatmap plot showing the changed expression levels of overlapped genes from A. (C) Sequenced reads density plot showing the Chromatin Immunoprecipitation-sequencing signal of USF1 on NEAT1 genomic location. (D) Bar plot showing the suppressed expression level of NEAT1 by USF1-overexpression in Huh7 cells. ***P<0.001. (E) Box plot showing the expression level of NEAT1 in LIHC patients. *P<0.05. (F) Line plot showing the prognostic results by dividing patients with LIHC into two groups according to NEAT1 expression levels. USF1, upstream transcription factor 1; DEGs, differentially expressed genes; LIHC, liver hepatocellular carcinoma; FPKM, fragments per kilobase of transcript per million fragments mapped.

by NF-κB inactivation (32). In HCC, the inflammation can be orchestrated by the tumor itself by secreting factors that recruit inflammatory cells to the tumor favoring the buildup of a microenvironment, and inflammation promotes HCC development by promoting a series of cancer-promoting biological processes (33). At present, immunotherapies have shown their
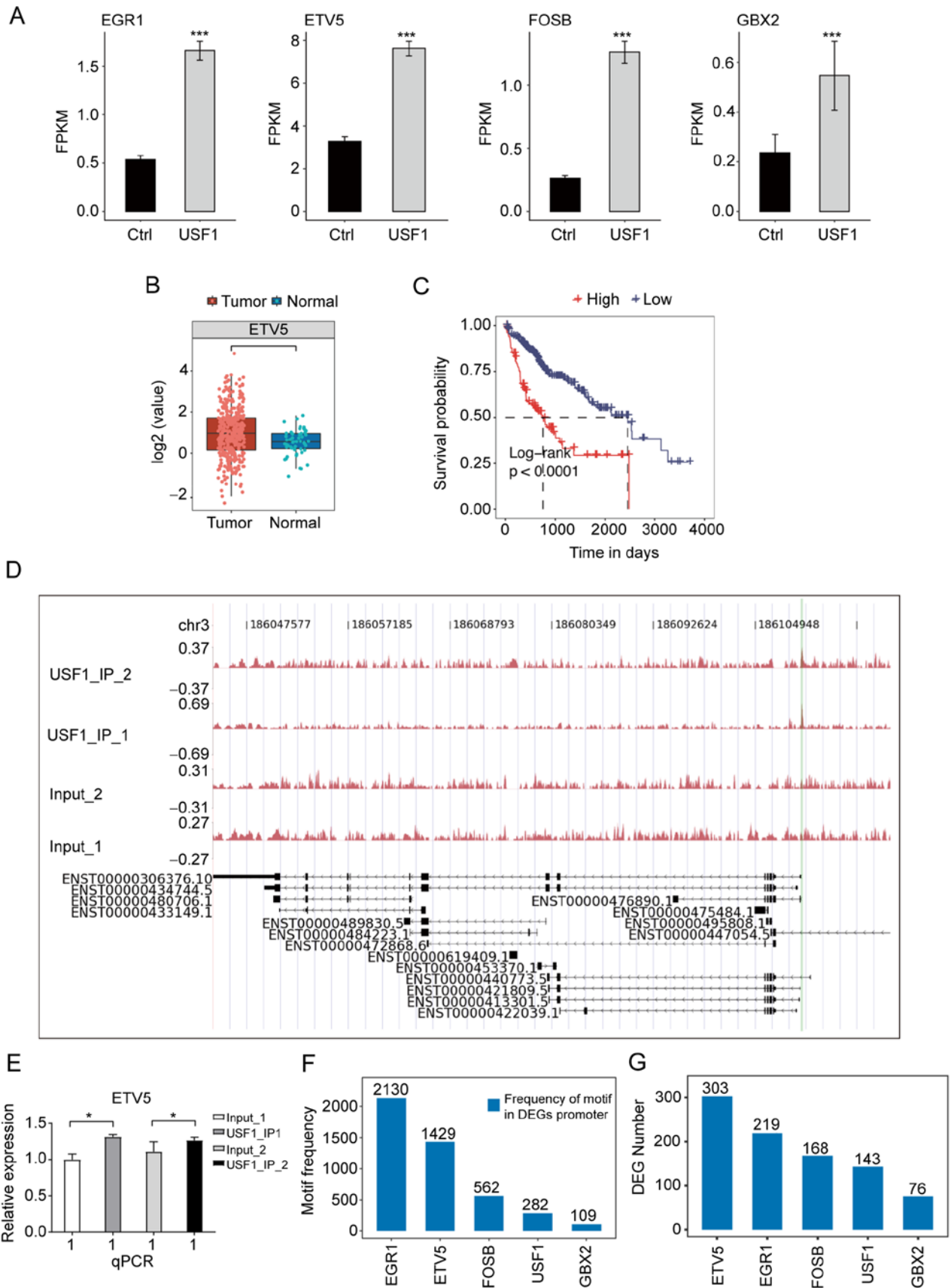
Figure 6. USF1 modulates gene expression by regulating TFs in Huh7 cells. (A) Bar plot showing the expression levels of four differentially expressed TFs bound by USF1. (B) Box plot showing the expression level of ETV5 in patients with LIHC. (C) Line plot showing the prognostic results by dividing patients with LIHC into two groups according to ETV5 expression levels. (D) Sequenced reads density plot showing the ChIP-sequencing signal of USF1 on ETV5 genomic location. (E) Bar plot showing the ChIP-qPCR validation result for USF1 binding site on the promoter region of ETV5. (F) Bar plot showing the motif number on the promoter region of USF1-regulated DEGs for the five TFs. (G) Bar plot showing the DEG number with binding motifs from Fig. 6F for the five TFs. $^*P<0.05$ and $^{***}P<0.001$ using Student's t-test. USF1, upstream transcription factor 1; TFs, transcription factor; LIHC, liver hepatocellular carcinoma; ChIP, Chromatin Immunoprecipitation; qPCR, quantitative PCR; DEGs, differentially expressed genes.

advantages in HCC treatment and several other cancer immuno-therapies are also in early-stage clinical trials for the treatment of advanced HCC (34). Among the upregulated DEGs, several chemokine and interleukin genes were detected, including CXCL1, CXCL3, CXCL10, CXCL11, IL1A, IL1B and IL6, several of which were associated with the progression of HCC. A previous study demonstrated that in HCC cells, CXCL1 is secreted in response to metabolic syndrome signals and may promote the progression of HCC through apoptosis recovery or the metastasis pathway (35). IL6 cooperates with IL6R and triggers the activation of the JAK-STAT3 signaling pathway, which could participate in the processes of anti-apoptosis, angiogenesis, proliferation, invasion, metastasis and drug resistance of cancer cells (36). In HCC cells, it was found that CXCL3 and CD133 form a positive feedback loop to maintain the CD133^{+} cancer stem cell populations via Erk1/2 activation, indicating the potential of CXCL13 as a therapeutic target for HCC (37). It was hypothesized that USF1 could promote HCC progression by upregulating the expression of these genes and modulating the immune microenvironment of tumor. Further studies are necessary to deeply explore how USF1 regulates the proportion and infiltration dysregulation, as well as gene expression alteration of immune cells in HCC.

The global interacting DNA targets of USF1 were then identified using ChIP-seq data and 2,492 target genes were detected. The canonical binding motifs of USF1 were identified, consistently with the previous result in the HepG2 cell line, a hepatoblastoma cell line, using the ChIP-chip method (5), indicating the high confidence of the ChIP-seq result. For the overlapped peak genes in the two replicates, it was found that they were enriched in several types of cancer and cancer-associated pathways, suggesting that USF1 may modulate HCC progression by affecting the transcription of cancer-associated genes. The most enriched GO Biological Process subontology pathway was the viral process; meanwhile, the pathogenesis of HCC is tightly associated with hepatitis B and C viral infections, especially for hepatitis B virus infection (38). The viral process-associated genes bound by USF1 indicated that USF1 may modulate the replication and functions of the hepatitis B or C virus to accelerate the progression of HCC. Multiple transcription regulation and RNA splicing pathways were also enriched, implying that USF1 binds to the promoter regions of TFs and splicing regulators. A previous study demonstrated that USF1 epigenetically modulates TF-HoxB4 transcription to control the lineage differentiation of embryonic stem cells (39). These downstream regulators of USF1 could also regulate their downstream targets, thus forming a multiple-level regulatory network of USF1; this regulatory network was reflected in the RNA-seq data of USF1. In addition to these pathways, autophagy, lysosome and apoptosis KEGG pathways were enriched by USF1-bound genes. USF1 was reported to suppress autophagy-related gene expression via positive regulation of mTOR transcription in HepG2 cells (40). In multiple cancer cell lines, including HepG2, USF1 could cooperate with RAD51 to regulate transcription of genes associated with the autophagy pathway, such as ATG3 and ATG5, by binding to their promoter regions (41), which was consistent with the present results. In summary, the present results suggested that USF1 could broadly bind to

the promoters of various cancer-associated genes in multiple cancer cell lines and USF1 probably plays important roles in the progression of multiple liver cancer types, including HCC and hepatoblastoma. As for the spatial and functional relationship between USFs and H3ac at protein-coding gene promoters (5), it was hypothesized that the inhibitors of histone deacetylase may modulate the functions of USF1 and thus these could be drug candidates in HCC by targeting USF1.

Lastly, an interaction analysis between DEGs and bound genes by USF1 was performed. However, only a few genes passed the criteria of both DEGs and USF1-bound genes, suggesting that USF1 may also indirectly regulate gene expression. Among the directly bound DEGs by USF1, several TFs were detected and focused on ETV5, which acts as an oncoprotein and is implicated in numerous cancers (42). ETV5 gene fusions with TMPRSS2 and SLC45A3 were detected in patients with prostate cancer, and ETV5 overexpression promoted the invasion of RWPE cells, indicating the biomarker potential of ETV5 in prostate cancer (43). In hepatocytes, ETV5 regulates hepatic fatty acid metabolism by binding to the PPAR response element region of downstream genes (44), indicating the critical role of ETV5 in liver diseases. In the present study, a dramatic increase in ETV5 expression by USF1-OE was detected. Meanwhile, the binding motif of ETV5 was presented in more DEGs than that of USF1 and other USF1-bound TFs, suggesting that ETV5 may directly regulate the expression of DEGs obtained through USF1-OE. These results could indicate that ETV5 is a target of USF1 and participates in the USF1-induced progression of HCC. The USF1-ETV5 regulatory axis may be treated as a target for HCC therapy in future.

There were certain limitations to the present study. Experiments performed on other HCC cell lines would strengthen the significance of the present results and conclusion. The experiments using *in vivo* animal models or more clinical cases could also provide more robust results for the important functions of USF1 in HCC. At the same time, the exact functions and molecular mechanisms of USF1 downstream targets, including NEAT1 and ETV5, could be identified using additional experiments in HCC cell lines, although there are several studies summarizing their functions in cancers. Thus, deeper studies are necessary to solve the aforementioned questions in future.

In conclusion, the present deeply investigated the downstream targets of USF1 and their potential functions associated with HCC in Huh7 cells. The present results demonstrated that USF1 binds to the promoter region of thousands of genes and significantly affects the expression of part genes. The downstream genes, including lncRNA-NEAT1 and TF-ETV5, may have essential regulatory functions in the USF1-regulated network and be involved in the progression of HCC. Further studies are also needed to deeply explore the underlying molecular mechanism and biological functions of USF1 and identify the potential value of USF1 for clinical treatment of HCC.

Availability of data and materials

All data generated or analyzed during this study are included in this published article. The datasets generated and/or analyzed during the current study are available in the Gene Expression Omnibus repository (https://www.ncbi.nlm.nih.gov/geo/query/acc.cgi?acc=GSE232263).

Authors' contributions

YLZ and FG conceived and designed the study, conducted experiments, analyzed the data and wrote the manuscript. PPR, CZ and LM participated in the study design, performed data analysis and provided critical revisions to the manuscript. XW and RW contributed to the experimental work, data interpretation and manuscript revisions. YK and KL provided technical support, performed data analysis and contributed to the manuscript preparation. All authors have read and approved the final version of the manuscript. YLZ and FG confirm the authenticity of all the raw data.

Ethics approval and consent to participate

Not applicable.

Patient consent for publication

Not applicable.

Competing interests

The authors declare that they have no competing interests.

References

1. Sung H, Ferlay J, Siegel RL, Laversanne M, Soerjomataram I, Jemal A and Bray F: Global cancer statistics 2020: GLOBOCAN estimates of incidence and mortality worldwide for 36 cancers in 185 countries. CA Cancer J Clin 71: 209-249, 2021.
2. Cao W, Chen HD, Yu YW, Li N and Chen WQ: Changing profiles of cancer burden worldwide and in China: A secondary analysis of the global cancer statistics 2020. Chin Med J (Engl) 134: 783-791, 2021.
3. Anwanwan D, Singh SK, Singh S, Saikam V and Singh R: Challenges in liver cancer and possible treatment approaches. Biochim Biophys Acta Rev Cancer 1873: 188314, 2020.
4. Nakagawa H, Fujita M and Fujimoto A: Genome sequencing analysis of liver cancer for precision medicine. Semin Cancer Biol 55: 120-127, 2019.
5. Rada-Iglesias A, Ameur A, Kapranov P, Enroth S, Komorowski J, Gingeras TR and Wadelius C: Whole-genome maps of USF1 and USF2 binding and histone H3 acetylation reveal new aspects of promoter structure and candidate genes for common human disorders. Genome Res 18: 380-392, 2008.
6. Lu TC, Wang Z, Feng X, Chuang P, Fang W, Chen Y, Neves S, Maayan A, Xiong H, Liu Y, et al: Retinoic acid utilizes CREB and USF1 in a transcriptional feed-forward loop in order to stimulate MKP1 expression in human immunodeficiency virus-infected podocytes. Mol Cell Biol 28: 5785-5794, 2008.
7. Zeng Y, Li H, Zhang X, Shang J and Kang Y: Basal transcription of APOBEC3G is regulated by USF1 gene in hepatocyte. Biochem Biophys Res Commun 470: 54-60, 2016.
8. Kim KC, Yun J, Son DJ, Kim JY, Jung JK, Choi JS, Kim YR, Song JK, Kim SY, Kang SK, et al: Suppression of metastasis through inhibition of chitinase 3-like 1 expression by miR-125a-3p-mediated up-regulation of USF1. Theranostics 8: 4409-4428, 2018.
9. Chang JTC, Yang HT, Wang TCV and Cheng AJ: Upstream stimulatory factor (USF) as a transcriptional suppressor of human telomerase reverse transcriptase (hTERT) in oral cancer cells. Mol Carcinog 44: 183-192, 2005.
10. Costa L, Corre S, Michel V, Le Luel K, Fernandes J, Ziveri J, Jouvion G, Danckaert A, Mouchet N, Da Silva Barreira D, et al: USF1 defect drives p53 degradation during Helicobacter pylori infection and accelerates gastric carcinogenesis. Gut 69: 1582-1591, 2020.
11. Song X, Zhu M, Li H, Liu B, Yan Z, Wang W, Li H, Sun J and Li S: USF1 promotes the development of knee osteoarthritis by activating the NF-κB signaling pathway. Exp Ther Med 16: 3518-3524, 2018.
12. Zhang L, Handel MV, Schartner JM, Hagar A, Allen G, Curet M and Badie B: Regulation of IL-10 expression by upstream stimulating factor (USF-1) in glioma-associated microglia. J Neuroimmunol 184: 188-197, 2007.
13. Wei G, Zhang T, Li Z, Yu N, Xue X, Zhou D, Chen Y, Zhang L, Yao X and Ji G: USF1-mediated upregulation of lncRNA GAS6-AS2 facilitates osteosarcoma progression through miR-934/BCAT1 axis. Aging (Albany NY) 12: 6172-6190, 2020.
14. Sun Q, Li J, Li F, Li H, Bei S, Zhang X and Feng L: LncRNA LOXL1-AS1 facilitates the tumorigenesis and stemness of gastric carcinoma via regulation of miR-708-5p/USF1 pathway. Cell Prolif 52: e12687, 2019.
15. Zhao X, Wang T, Liu B, Wu Z, Yu S and Wang T: Significant association between upstream transcription factor 1 rs2516839 polymorphism and hepatocellular carcinoma risk: A case-control study. Tumour Biol 36: 2551-2558, 2015.
16. Liu S, Qiu J, He W, Geng C, He G, Liu C, Cai D, Liu X, Tian B and Pan H: TUG1 long non-coding RNA enlists the USF1 transcription factor to overexpress ROMO1 leading to hepatocellular carcinoma growth and metastasis. MedComm (2020) 1: 386-399, 2020.
17. Peng JY, Cai DK, Zeng RL, Zhang CY, Li GC, Chen SF, Yuan XQ and Peng L: Upregulation of superenhancer-driven LncRNA FASRL by USF1 promotes de novo fatty acid biosynthesis to exacerbate hepatocellular carcinoma. Adv Sci (Weinh) 10: e2204711, 2022 (Epub ahead of print).
18. Chen B, Chen XP, Wu MS, Cui W and Zhong M: Expressions of heparanase and upstream stimulatory factor in hepatocellular carcinoma. Eur J Med Res 19: 45, 2014.
19. Kim D, Langmead B and Salzberg SL: HISAT: A fast spliced aligner with low memory requirements. Nat Methods 12: 357-360, 2015.
20. Trapnell C, Williams BA, Pertea G, Mortazavi A, Kwan G, van Baren MJ, Salzberg SL, Wold BJ and Pachter L: Transcript assembly and quantification by RNA-Seq reveals unannotated transcripts and isoform switching during cell differentiation. Nat Biotechnol 28: 511-515, 2010.
21. Robinson MD, McCarthy DJ and Smyth GK: edgeR: A Bioconductor package for differential expression analysis of digital gene expression data. Bioinformatics 26: 139-140, 2010.
22. Langmead B and Salzberg SL: Fast gapped-read alignment with bowtie 2. Nat Methods 9: 357-359, 2012.
23. Zhang Y, Liu T, Meyer CA, Eeckhoute J, Johnson DS, Bernstein BE, Nusbaum C, Myers RM, Brown M, Li W and Liu XS: Model-based analysis of ChIP-Seq (MACS). Genome Biol 9: R137, 2008.
24. Ramírez F, Ryan DP, Grüning B, Bhardwaj V, Kilpert F, Richter AS, Heyne S, Dündar F and Manke T: deepTools2: A next generation web server for deep-sequencing data analysis. Nucleic Acids Res 44 (W1): W160-W165, 2016.
25. Heinz S, Benner C, Spann N, Bertolino E, Lin YC, Laslo P, Cheng JX, Murre C, Singh H and Glass CK: Simple combinations of lineage-determining transcription factors prime cis-regulatory elements required for macrophage and B cell identities. Mol Cell 38: 576-589, 2010.
26. Livak KJ and Schmittgen TD: Analysis of relative gene expression data using real-time quantitative PCR and the 2(-Delta Delta C(T)) method. Methods 25: 402-408, 2001.

27. Tang Z, Kang B, Li C, Chen T and Zhang Z: GEPIA2: An enhanced web server for large-scale expression profiling and interactive analysis. Nucleic Acids Res 47 (W1): W556-W560, 2019.
28. Nagy Á, Munkácsy G and Győrffy B: Pancancer survival analysis of cancer hallmark genes. Sci Rep 11: 6047, 2021.
29. Corre S and Galibert MD: Upstream stimulating factors: Highly versatile stress-responsive transcription factors. Pigment Cell Res 18: 337-348, 2005.
30. Dong P, Xiong Y, Yue J, Hanley SJB, Kobayashi N, Todo Y and Watari H: Long non-coding RNA NEAT1: A novel target for diagnosis and therapy in human tumors. Front Genet 9: 471, 2018.
31. Tiruppathi C, Soni D, Wang DM, Xue J, Singh V, Thippegowda PB, Cheppudira BP, Mishra RK, Debroy A, Qian Z, et al: The transcription factor DREAM represses the deubiquitinase A20 and mediates inflammation. Nat Immunol 15: 239-247, 2014.
32. Cho MJ, Lee DG, Lee JW, Hwang B, Yoon SJ, Lee SJ, Park YJ, Park SH, Lee HG, Kim YH, et al: Endothelial PTP4A1 mitigates vascular inflammation via USF1/A20 axis-mediated NF-κB inactivation. Cardiovasc Res 119: 1265-1278, 2023.
33. Yu LX, Ling Y and Wang HY: Role of nonresolving inflammation in hepatocellular carcinoma development and progression. NPJ Precis Oncol 2: 6, 2018.
34. Liu JKH, Irvine AF, Jones RL and Samson A: Immunotherapies for hepatocellular carcinoma. Cancer Med 11: 571-591, 2022.
35. Dahlquist KJV, Voth LC, Fee AJ and Stoeckman AK: An autocrine role for CXCL1 in progression of hepatocellular carcinoma. Anticancer Res 40: 6075-6081, 2020.
36. Xu J, Lin H, Wu G, Zhu M and Li M: IL-6/STAT3 is a promising therapeutic target for hepatocellular carcinoma. Front Oncol 11: 760971, 2021.
37. Zhang L, Zhang L, Li H, Ge C, Zhao F, Tian H, Chen T, Jiang G, Xie H, Cui Y, et al: CXCL3 contributes to CD133(+) CSCs maintenance and forms a positive feedback regulation loop with CD133 in HCC via Erk1/2 phosphorylation. Sci Rep 6: 27426, 2016.
38. Ringelhan M, McKeating JA and Protzer U: Viral hepatitis and liver cancer. Philos Trans R Soc Lond B Biol Sci 372: 20160274, 2017.
39. Deng C, Li Y, Liang S, Cui K, Salz T, Yang H, Tang Z, Gallagher PG, Qiu Y, Roeder R, et al: USF1 and hSET1A mediated epigenetic modifications regulate lineage differentiation and HoxB4 transcription. PLoS Genet 9: e1003524, 2013.
40. Guo J, Fang W, Chen X, Lin Y, Hu G, Wei J, Zhang X, Yang C and Li J: Upstream stimulating factor 1 suppresses autophagy and hepatic lipid droplet catabolism by activating mTOR. FEBS Lett 592: 2725-2738, 2018.
41. Kang K, Choi Y, Moon H, You C, Seo M, Kwon G, Yun J, Beck B and Kang K: Epigenomic analysis of RAD51 ChIP-seq data reveals cis-regulatory elements associated with autophagy in cancer cell lines. Cancers (Basel) 13: 2547, 2021.
42. Oh S, Shin S and Janknecht R: ETV1, 4 and 5: An oncogenic subfamily of ETS transcription factors. Biochim Biophys Acta 1826: 1-12, 2012.
43. Helgeson BE, Tomlins SA, Shah N, Laxman B, Cao Q, Prensner JR, Cao X, Singla N, Montie JE, Varambally S, et al: Characterization of TMPRSS2:ETV5 and SLC45A3:ETV5 gene fusions in prostate cancer. Cancer Res 68: 73-80, 2008.
44. Mao Z, Feng M, Li Z, Zhou M, Xu L, Pan K, Wang S, Su W and Zhang W: ETV5 regulates hepatic fatty acid metabolism through PPAR signaling pathway. Diabetes 70: 214-226, 2021.